Modelling and simulation of vibratory driven sheet piles - development of a stop criterion

Anton Andersson [i)], Johannes Jonsson [i)], Kenneth Viking [ii)], Erika Tudisco [iii)] and Per-Erik Austrell [iv)]

i) MSc, Department of Civil Engineering, Lund University, Sweden

ii) Ph.D, Geotechnician, Swedish Transport Administration (Trafikverket), Stockholm, Sweden.

iii) Associate professor, Division of Geotechnical Engineering, Department of Construction Sciences, Lund University, Sweden.

iv) Professor, Division of Structural Mechanics, Department of Construction Sciences, Lund University, Sweden.

ABSTRACT

During excavations, steel sheet piles are often installed through vibratory driving. This is especially effective in soft soils. However, when installing sheet piles in other soils such as glacial till, there is a risk of impact with boulders that may damage the sheet pile toe. This may result in unnecessary time- and cost intensive measures to ensure stable and watertight excavation. Hence, there is a need for a criterion to stop the driving before the sheet pile is severely damaged. The purpose of this paper is to investigate how numerical models may be used to simulate a sheet pile encountering a boulder during vibratory driving, and to investigate the possibility of developing a stop criterion based on the outcome of the models. Two numerical models were created to simulate the vibratory driving: a uniaxial multi degree of freedom model and a finite element (FE) model, by using the numeric platform MATLAB and the FE software ABAQUS respectively. The simulations were carried out through explicit time integration in both models. The external actions on the sheet pile, i.e., the vibratory driving force, soil resistance and obstacle resistance were estimated with methods found in literature. The models were then calibrated against a field study by using its results as input to the models. The encounter with a boulder, was simulated in different ways. In the uniaxial model, the contact was modeled by an elastoplastic contact force and in the FE model a solid body with high stiffness was introduced. The results of the numerical models show promising resemblance with the results of the field study. Both the global driving speeds and the accelerations of the sheet pile corresponds well with the field study for both models. The simulations indicate that boulder impacts may be detected by monitoring changes in acceleration amplitude traveling along the sheet pile. This suggest that a stop criterion for vibratory driving could be based on abrupt changes in acceleration amplitude. By creating a device with accelerometers detecting a significant increase in acceleration amplitude, damage to the sheet pile could be prevented. Although it should be mentioned that at weak impact points of the sheet pile cross section only small changes in the accelerations were seen in the simulations.

Keywords: sheet piles, vibratory driving, numerical modelling, finite element simulations, stop criterion

1 INTRODUCTION

Retaining walls are formed by interlocked sheet piles and are used to prevent soil instability and ground water leakage during excavation. A common way of installing the sheet piles is by driving them with a vertical vibratory motion, being especially convenient when sheet piles are driven through soft soil. However, in many parts of the northern hemisphere, the ground consists of glacial till, generally very compact and containing a large range of grain sizes. Large grains such as cobbles and boulders are common. Thus, there is a risk of impact with boulders as shown in Figure 1. The pile cross section is also shown in the figure. Damage to the sheet piles can be very costly and time-consuming. Additional measures are needed to ensure stability and water tightness as a result of the damage. Hence, there is a need to detect hazardous situations, and to stop the driving before the sheet pile is severely damaged. Finding a criterion to shut down the driving is thus of high priority.

The purpose of this paper is to investigate how numerical models may be used to simulate vibratory driving of a sheet pile, including situations where rigid objects are encountered, and to investigate the possibility of developing a stop criterion based on these numerical simulations.

Two different models were created: a uniaxial multi degree of freedom model, and a finite element (FE) model. The reason for using two models of different complexity was to be able to check the models against each other.

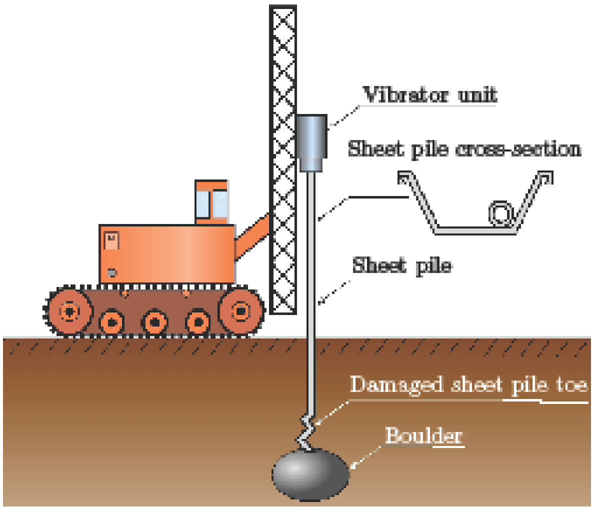

Fig. 1. Vibratory driving device and sheet pile cross section.

Also, the uniaxial model has comparatively few degrees of freedom and can thus be run rapidly in parameter studies.

The models were calibrated against an experimental field study of sheet pile vibratory driving (Viking, 2002). Thereafter, a rigid obstacle was introduced into the models, to simulate the effects of an impact during vibratory driving. The resulting compressive accelerations from the impacts were then used to draw conclusions regarding a potential stop criterion.

The numerical platform MATLAB was used to create the uniaxial model, and for performing simulations. Spring like elements were used for the sheet pile and the impact with the boulder was modeled using an elastoplastic contact force. Studies of the vibratory parameters were conducted to gain better understanding of the dynamics in the vibratory driving process using this simple model.

The more complex FE model was developed using the software ABAQUS with shell elements for the sheet pile. The boulder impact was obtained by driving the sheet pile into a solid sphere with high modulus of elasticity. It was also decided that explicit time-integration was to be used to run the simulations in both models. Moreover, the resistance from the surrounding soil was in both cases modeled by discrete elastoplastic elements along the sheet pile.

The disposition of the paper is as follows: after this introduction, Section 2 will cover the basics of a vibratory driving forces, while soil resistance, and the results from the field tests are dealt with in Section 3. The FE model and the uniaxial model are presented in Section 4 and results in Section 5. Finally, in Section 6, a summary and suggestions for future work are given.

2 FORCES IN VIBRATORY DRIVING

There are two basic ways to vibrate piles into the ground. The one studied here is shown in Figure 1 and is a leader-mounted system. The other system is a free-hanging system.

The force $F_d = F_0 + F_v$ generated by the vibro unit, driving the sheet pile can be expressed as sum of a static and a dynamic force where F_0 is the static force from the total weight resting on the sheet pile as well as the force exerted by the leader mast (illustrated as a truss structure in Figure 1). This part of the force can be directed either up- or downwards. In a free-hanging system the downward directed force cannot be greater than the weight. The dynamic force F_v is sinusoidal according to Figure 2 (also showing the static force).

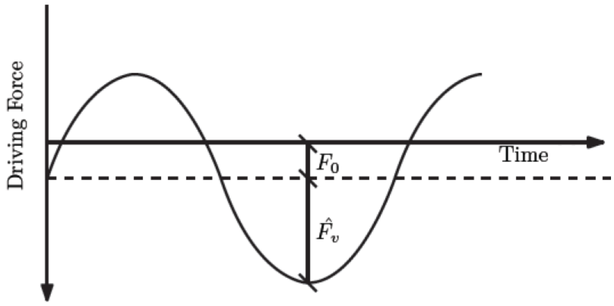

Fig. 2. Driving force of a leader system; sum of a static and a dynamic part.

The dynamic force has the amplitude $\hat{F}_v$ and this part of the force is accomplished by two rotating eccentric masses. These are rotating in different directions, in order to cancel the horizontal dynamic force, as shown in Figure 3.

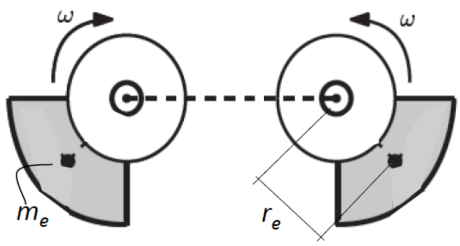

Fig. 3. Rotating eccentric masses in the vibrator unit.

The dynamic vertical force amplitude $\hat{F}_v = m_e \cdot r_e \cdot \omega^2$ depends on the eccentric mass m_e, the eccentricity r_e, and the angular velocity ω. The quantity $M_e = m_e \cdot r_e$ is called the eccentric moment.

3 SOIL RESISTANCE

Soil liquefaction is claimed to be the main reason for vibratory driving being such an effective installation method for piles. The soil shear strength is reduced due to the soil grains being moved rapidly and the generated pore water pressure reduces the contact forces between the grains. Despite these key factors, it’s the cone penetration test (CPTu) that’s often used to establish dynamic soil resistance properties. In the CPTu test a bar with a conical tip is pressed down into the ground with a constant velocity of 20mm/s. The quasi-static data from this test are then converted into dynamic soil resistance applicable to the up and down motion in about 40Hz often used in vibratory driving. The procedure for converting CPTu test data to dynamic soil resistance is not described here. See (Andersson and Jonsson, 2021, Section 2.5.3) for a detailed description. Finally, an elastoplastic (frictional) soil resistance model is calibrated to the converted values as described below.

3.1 Dynamic soil resistance from field test

The dynamic pressure stress q_d on the cross section of the toe and the dynamic shear stress τ_d (friction) along the sheet pile surface are called dynamic toe resistance and dynamic shaft resistance, respectively.

In Figure 4 these quantities are shown as functions of piling depth.

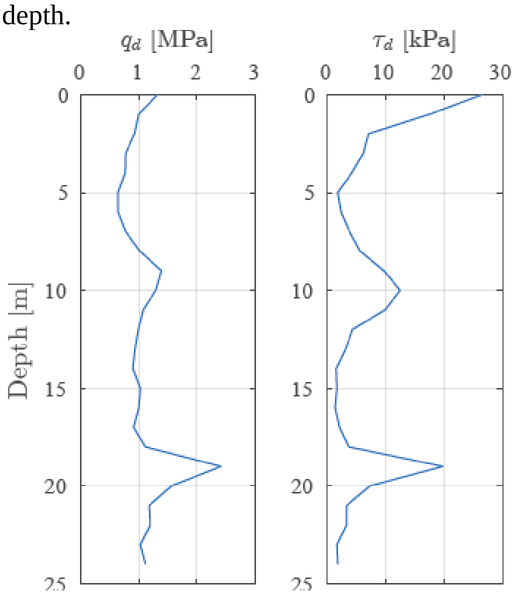

Fig. 4. Dynamic toe and shaft resistance vs depth.

The pressure stress on the toe is higher than the frictional shear stress on the shaft. However, the surface that the shear stress act upon is much larger.

3.2 Soil resistance model

The pressure and shear stresses on the sheet pile shown in Figure 4 are integrated over the surfaces they act on to establish the resisting forces on the sheet pile. The perimeter of sheet pile is Ω_p and A_p is the cross section area of the sheet pile, while z is a depth measure.

$$R_{s,max} = \Omega_p \int_0^z \tau_d \, dz \tag{1}$$

$$R_{t,max} = q_d(z) A_p \tag{2}$$

The resulting forces $R_{s,max}$ and $R_{t,max}$ should be considered as dynamic soil resistance forces acting on limited depth sections (1m) of the sheet pile. The reason for this is that the soil conditions affecting the upper part of the pile can be quite different from those at a lower part, as seen in Figure 4. The next step is to create a model that can take care of the dynamic resistance from the soil, that is acting all along the pile. However, in the models in Section 4, soil resistance act in discrete points (1m apart). The shaft resistance force R_s and the toe resistance force R_t depend on dynamic displacement u are according to an elastoplastic soil model shown in Figure 5. (Increasing u means that the pile is going deeper.)

The maximum forces developed in the dynamic action are given by Eq. (1) and (2) and vary discretely with depth z. The displacements Q_s and Q_t mark the limits of elastic behavior.

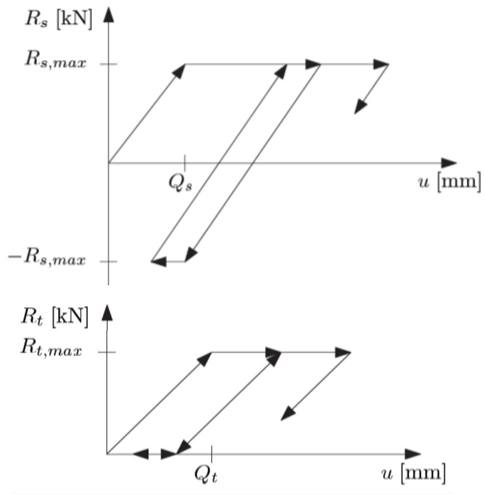

Fig. 5. The soil resistance force development versus displacement at a particular depth.

Hysteretic behavior is shown, due to the frictional properties of the soil, as displacement increase and decrease in the vibratory motion. Note the difference between shaft and toe resistance. As the displacement get smaller after the turning point, the toe resistance will eventually become zero as the tip is temporarily lifted from its current lowest position.

The pile is considered to be elastic and flexible so the dynamic displacement u is different at different depths z.

4 MODELS

As mentioned, two models were developed: a FE-model and a uniaxial model. Their interaction with the discrete soil resistance in Section 3 as well as the encounter with an obstacle, are described in this section. Figure 6 shows an overview of the models. The soil resistance model is only displayed in the uniaxial model but is also included in the FE model.

Both models were run with and without impacting an obstacle. The impact was simulated by contact using a rigid sphere in the FE model and using an elastoplastic contact force in the uniaxial model. The level of this force was taken from the simulations of impact in the FE model. This was done due to lack of field test data. However, some data (not used here) with limited impact and damage are given by (Guillemet, 2013).

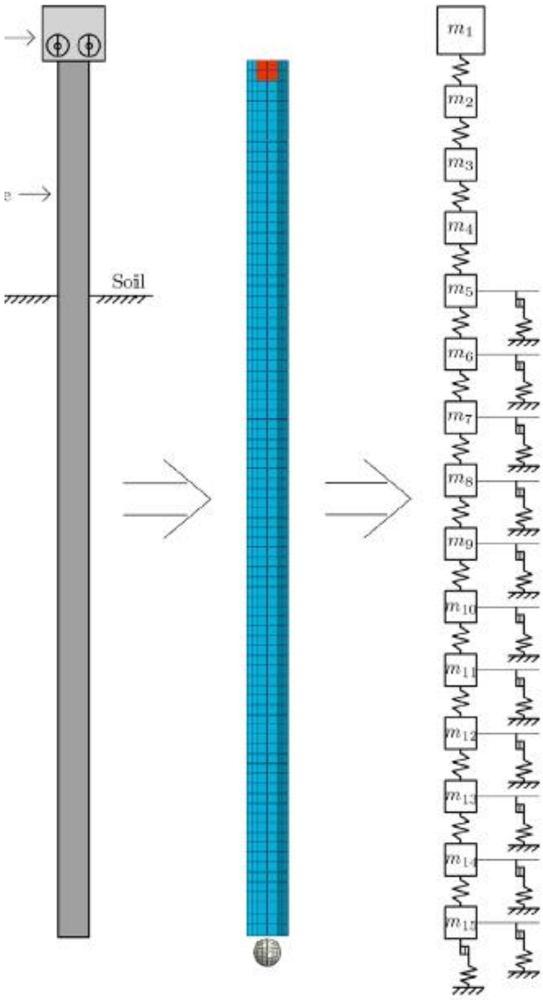

Fig. 6. Overview of the modelling including soil resistance.

4.1 The FE-model

The sheet pile, the spherical obstacle, and the discrete soil resistance according to Figure 6 were modelled in the commercial FE program ABAQUS Explicit. Shell elements (S4R with linear interpolation and reduced integration) were used for the pile, with an elastoplastic material model and parameters for steel (Young's modulus 210GPa, Yield stress 355MPa, and density 7800kg/m^3). The width of the steel sheet pile is 0.6m, depth 0.23 m, and the length of the pile was set to 14m. The (simplified) cross section of the pile is shown in Figure 7.

The obstacle was modeled as a solid sphere with a diameter of 0.4m and parameters for granite (C3D8R elements with Young's modulus 50GPa).

Shaft resistance (soil shear strength) was obtained by the use of so called connector elements placed at intervals of one meter and mimicking the behavior of R_s in Figure 5. The toe resistance is much smaller than the shaft resistance in the case of normal driving without obstacles. This part of the soil resistance was therefore neglected in the normal driving mode.

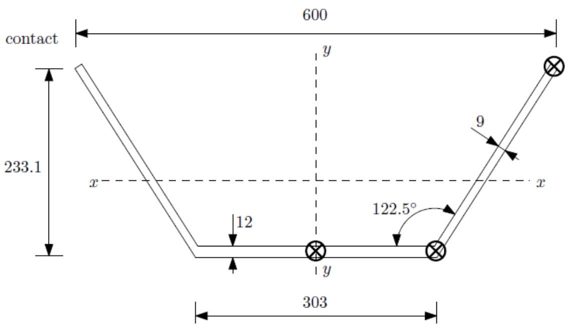

Fig. 7. The simplified cross section of the steel sheet pile including contact points with the obstacle.

Lateral displacements of the pile was prevented by displacement boundary conditions making the soil model completely stiff in this direction only giving resistance in the axial direction from the soil. This was done because the lateral displacements were judged to have no significant effect on the ability to drive the pile into the ground (Lund Tebäck, 2019). It does also simplify the modelling a lot.

Loads according to Figure 2 was applied as surface traction in the red area of the pile in Figure 6.

Damping in form of small Rayleigh β-damping was also added to the FE-model to get a damping ratio ζ of about 1% to eliminate some of the influence of high frequencies in the simulation making it possible to take longer time steps.

A convergence test in terms of element size was performed. An element size of 50mm (quadratic elements) in the sheet pile was found small enough except for a part near the sheet pile toe were the size was set to 25mm due to the deformations in the contact with the obstacle. Concerning the length of time steps it was handled automatically by ABAQUS explicit in order to stay below the stability limit. The time step is also adjusted due to energy conditions in ABAQUS. The total energy in the model should remain constant. If not the time step need to be smaller.

The contact force between the boulder (sphere) and the pile was determined by a quasi-static analysis in velocity control. The boulder was driven into one meter of the lowest part of the pile with a low constant velocity to a deformation of 30mm. By reversing velocity, the pile was then unloaded. This type of analysis can be done because the part of the pile at the toe were almost all displacement is taking place is small and has negligible inertia. Also no viscous effects are assumed in the elastoplastic buckling of the toe of the pile thus giving the same contact force as in a dynamic analysis.

Three cases of contact were studied according to Figure 7. The corner point between the web and the flange turned out to be stiffest with a maximum force of about 600KN and the point at the edge of the flange was the weakest point with a maximum value of about 100kN.

The point in the middle of the web gave a load displacement curve due to elastoplastic buckling according to Figure 8.

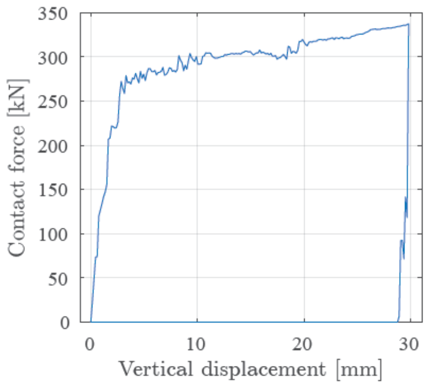

Fig. 8. Quasi-static contact force when the obstacle is pressed into the mid-point of the web.

In this case the force is still increasing as 30mm deformation is reached and the maximum value is about 350kN and thus between the other values.

It is an interest in itself to evaluate contact forces between boulder and pile. However, an idealized version of the curve in Figure 8 is also used in the uniaxial model to simulate the boulder impact by replacing it with a contact force.

4.2 The uniaxial - model

The uniaxial model is made up of spring like (bar) elements and discrete (lumped) masses in the nodes according to Figure 6, with nodes placed one meter apart.

The shaft resistance R_s was implemented with springs and frictional sliders giving a behavior as seen in Figure 5 with Q_s=2.8mm at all depths. The value of $R_{s,max}$ varies with depth according to Eq. (1). The toe resistance is negligible in normal driving but when hitting a boulder it is set to $R_{t,max}$=300kN being the (idealized) average of values in Figure 8 and the onset of plastic behavior is set to Q_t =3mm.

The model was as mentioned run in MATLAB with explicit time stepping using the Central difference method. The time step was set to 5 micro seconds after a convergence test.

5 RESULTS

Results from the field tests and model simulations are presented and discussed here. In the first part normal driving simulations without obstacles are compared to field test results. The second part concerns only simulated results as the pile encounters a boulder, due to lack of field test data. Further results and details are given in (Andersson and Jonsson, 2021).

5.1 Simulations vs test data – normal driving

Downward displacement and accelerations vs time were measured at 2, 6 and 10m penetration depth in a field study (Viking, 2002). An instrumented 14m long sheet pile with cross section as in Figure 7 was driven into a sandy soil without encountering major obstacles. The frequency was set to 41Hz and the eccentric moment (c.f. Section 2) was about 6kgm. The downward displacement in each cycle is about 5mm while the corresponding upwards displacement is about 2.5mm. In Figure 9 displacements are plotted against time at 6m penetration depth, measured 1m below the pile head. The graphs are from above: measurements, FE-model, and uniaxial model. For the model simulations soil data presented in Section 3 were used.

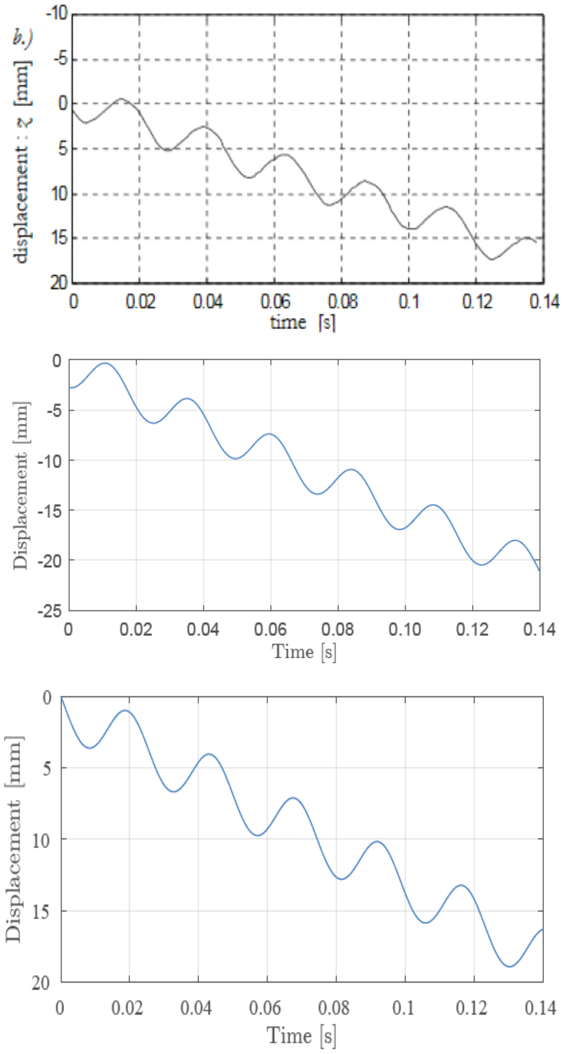

Fig. 9. Displacement development vs time at 6m penetration depth. From above: measurements, FE, and uniaxial model.

Simulations and measurement show quite similar behavior although there are some small differences. Also between the models there are some small differences.

Accelerations at 6m penetration depth were also measured at 1m below the pile head. Results are given in Figure 10. Again the results from the simulations show good resemblance with measurements.

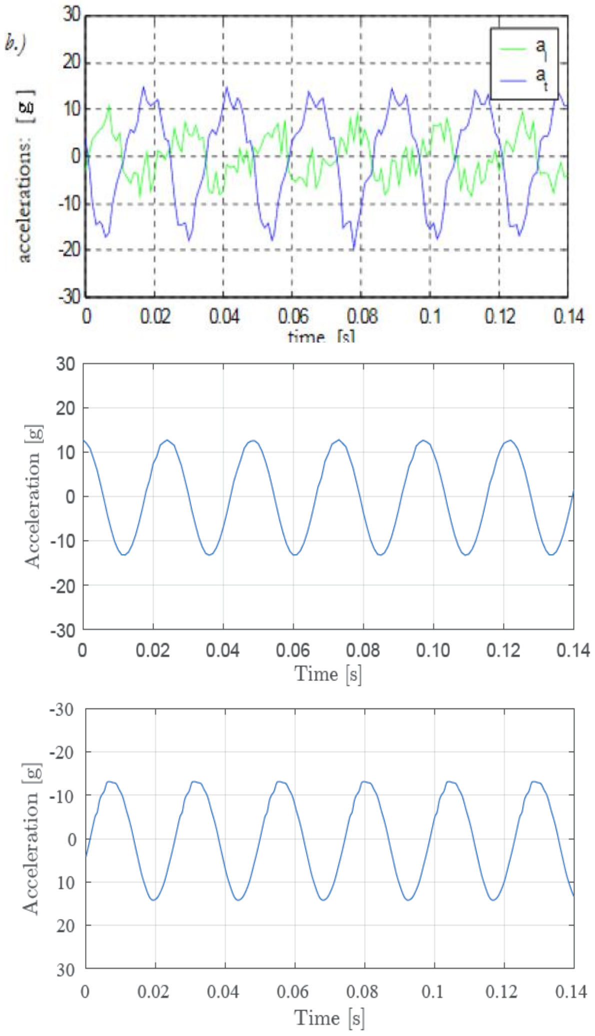

Fig. 10. Accelerations vs time at 6m penetration depth. From above: measurements, FE-model, and uniaxial model.

5.2 Model results for impact with boulder

Impact with a boulder was simulated with both models but could not be compared to measurements as mentioned before. However, the accelerations (rather than the displacements) obtained from the models are of interest due to their significant change after impact. The case in Section 4.1 with impact in the middle of the web show accelerations for the FE-model as given in Figure 11. The impact is simulated at 10m penetration depth and accelerations are monitored 1m below the pile head. The uniaxial model shows similar results. The figure show accelerations before and after impact, with a substantial change that could be used for stopping the driving before damaging the sheet pile too much. A device coupled to the pile head measuring accelerations could thus be used for the purpose. Accelerations double in amplitude at an impact in the middle of the web.

This also holds for the corner between web and flange. However, a bit disappointing, for impact at the edge of the flange (c.f. Figure 7) i.e. at the weakest spot, there were hardly any change seen in acceleration amplitude after impact.

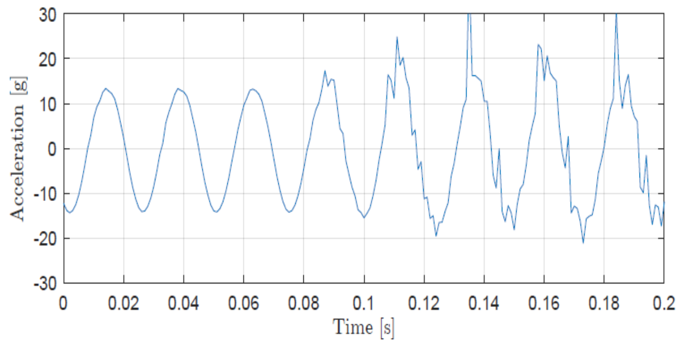

Fig. 11. Accelerations after hitting a boulder at the midpoint of the pile web.

6 CONCLUSIONS AND FUTURE WORK

The simulations performed in this work show good resemblance with the field measurements in terms of displacements and accelerations. Particularly the change in acceleration amplitudes are promising for the development of a stop-driving criterion to avoid damaging the steel sheet pile. Although, when impact occurred at the weakest point of the cross-section no significant acceleration changes could be seen. In a future work lateral displacements of the pile will also be investigated to see if these bending mode vibrations can be useful for a stop-driving criterion. It would also be interesting to develop a dynamic test method to replace the CPTu test used for the soil resistance in this study.

ACKNOWLEDGEMENTS

This paper is based on a master thesis work by Andersson and Jonsson, (2021), that was initiated by Viking (at the Swedish Transport Administration). He also conducted the field test described in Section 3.

REFERENCES

1) Andersson A. and Jonsson J., (2021): Modelling and simulation of vibratory driven sheet piles - development of a stop a criterion, Report TVSM-5254, Master Thesis, Structural Mechanics, Lund University, Sweden
2) Guillemet C. (2013); Pile–Soil Interaction during Vibratory Sheet Pile Driving -a Full Scale Field Study. Master Thesis, Civil and Architectural engineering, KTH, Stockholm, Sweden.
3) Lund Tebäck R. , (2019): Dynamisk Finita element-analys av vibrodriven spontplanka (in swedish), Report TVGT-5066, Master Thesis, Geotechnical Engineering, Lund University, Sweden
4) Viking K. (2002): Vibro-driveability - a field study of vibratory driven sheet-piles in non-cohesive soils. PhD Thesis, Civil and Architectural engineering, KTH, Stockholm, Sweden.